

ARTICLE

**Electronic supplementary information**

*for*

**Red-emitting neutral rhenium(I) complexes bearing a pyridyl pyridoannelated N-heterocyclic carbene**

Anna Bonfiglio,<sup>a</sup> Kevin Magra,<sup>b,\*<sup>a</sup></sup> Cristina Cebrián,<sup>b</sup> Federico Polo,<sup>c</sup> Philippe C. Gros,<sup>b,d</sup> Pierluigi Mercandelli,<sup>e</sup> and Matteo Mauro<sup>a</sup>

<sup>a</sup> Université de Strasbourg & CNRS, Institut de Physique et Chimie des Matériaux de Strasbourg (IPCMS), 23, rue du Loess, F-67034 Strasbourg (France), e-mail: [mauro@unistra.fr](mailto:mauro@unistra.fr)

<sup>b</sup> Université de Lorraine, CNRS, L2CM, F-57000 Metz (France)

<sup>c</sup> Department of Molecular Sciences and Nanosystems, Ca' Foscari University of Venice. Via Torino 155, 30172 Venezia (Italy)

<sup>d</sup> Université de Lorraine, CNRS, L2CM, F-54000 Nancy (France)

<sup>e</sup> Dipartimento di Chimica, Università degli Studi di Milano, via Camillo Golgi 19, 20133 Milano (Italy)

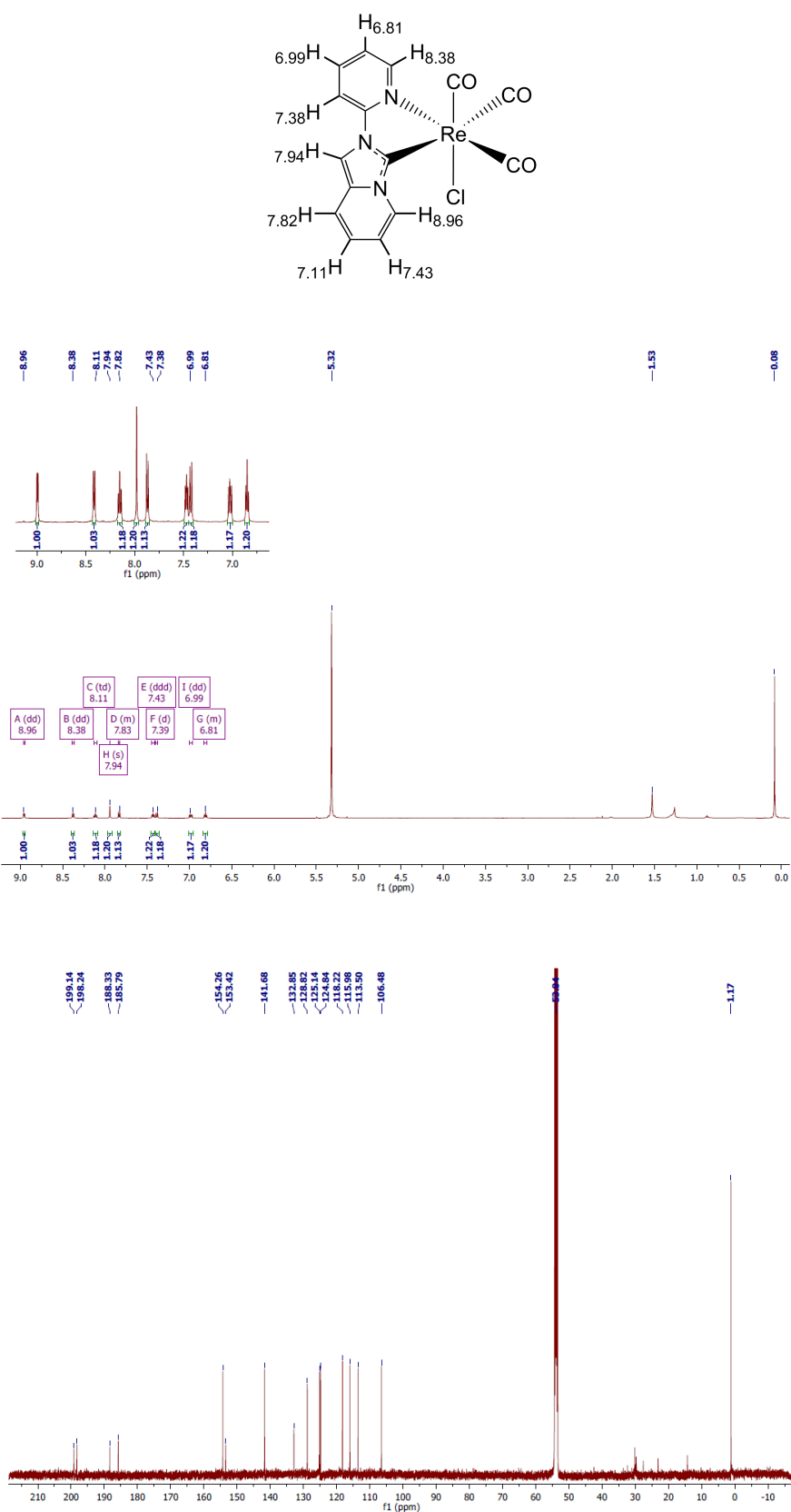


**Figure S1.** <sup>1</sup>H (500 MHz, top) and <sup>13</sup>C NMR (125 MHz, bottom) spectra recorded for complex **1** in CD<sub>2</sub>Cl<sub>2</sub> at 298 K.

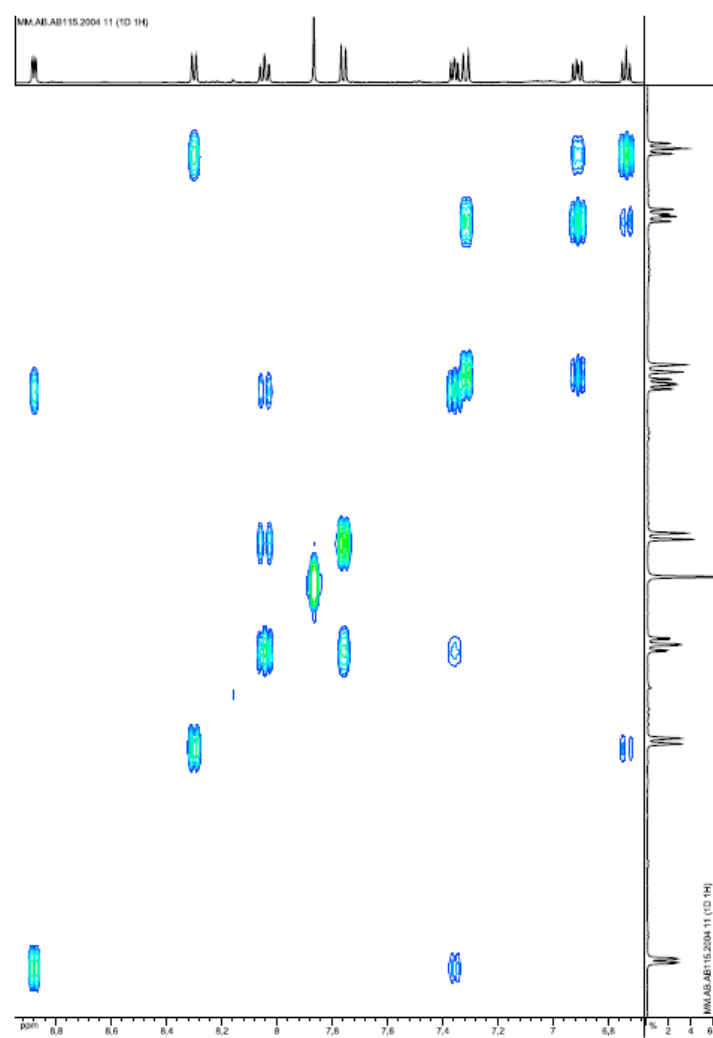


**Figure S2.** <sup>1</sup>H-<sup>1</sup>H COSY NMR spectrum recorded for complex **1** in CD<sub>2</sub>Cl<sub>2</sub> at 298 K.

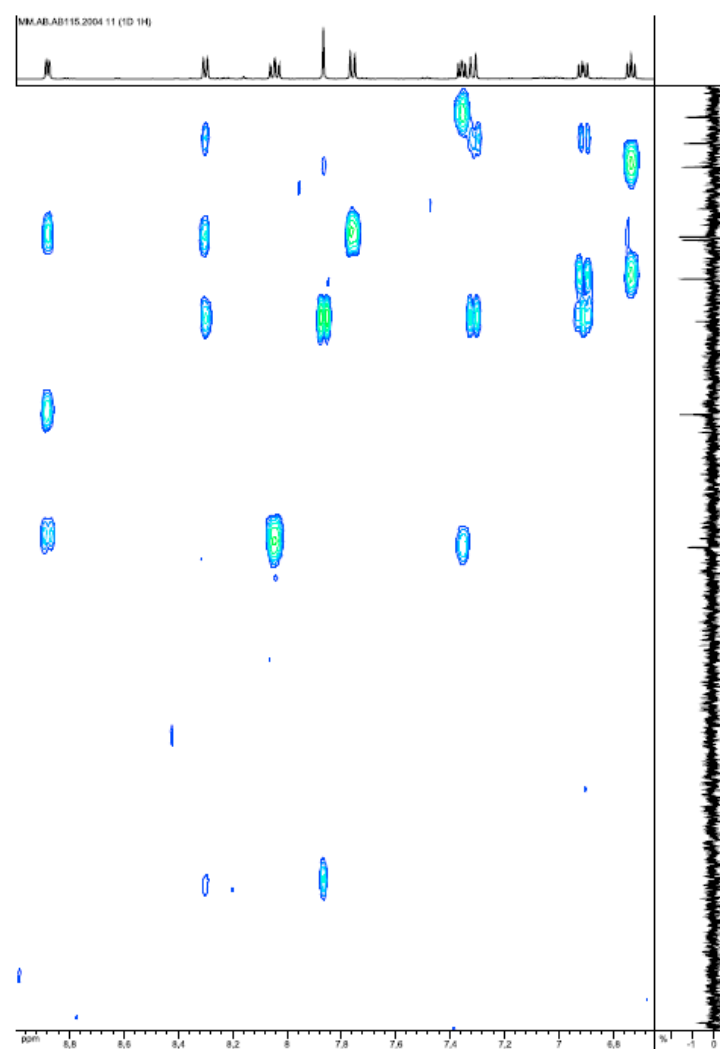


**Figure S3.**  $^1\text{H}$ - $^{13}\text{C}$  HMBC NMR spectrum recorded for complex **1** in  $\text{CD}_2\text{Cl}_2$  at 298 K.

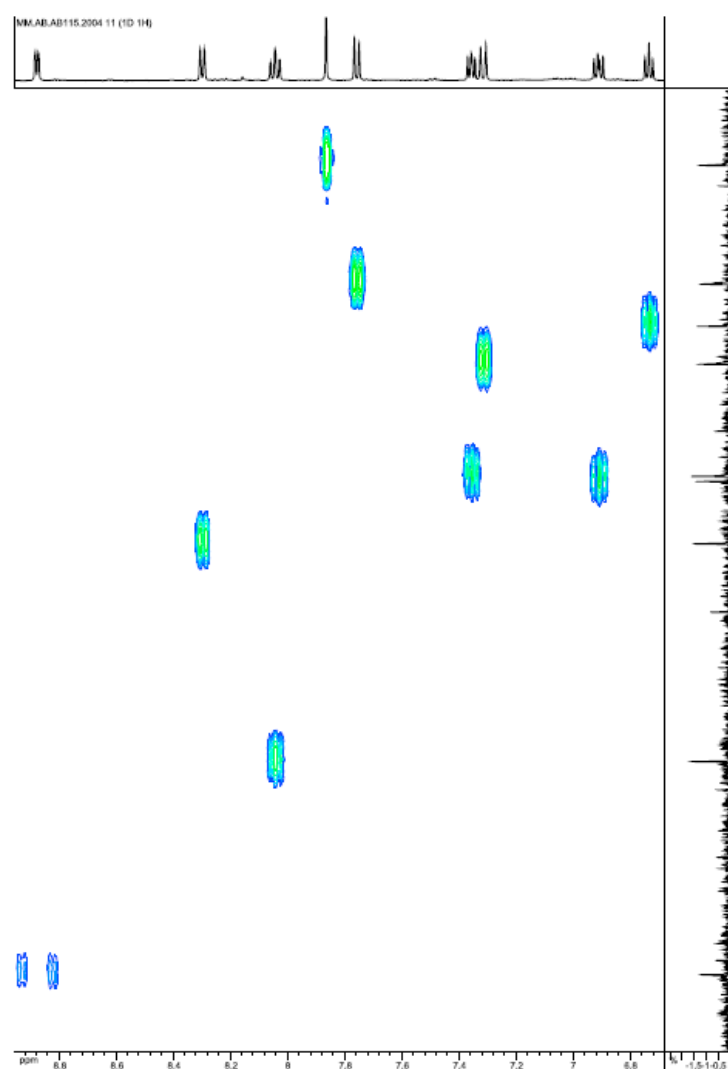


**Figure S4.** <sup>1</sup>H-<sup>13</sup>C HSQC NMR spectrum recorded for complex **1** in CD<sub>2</sub>Cl<sub>2</sub> at 298 K.

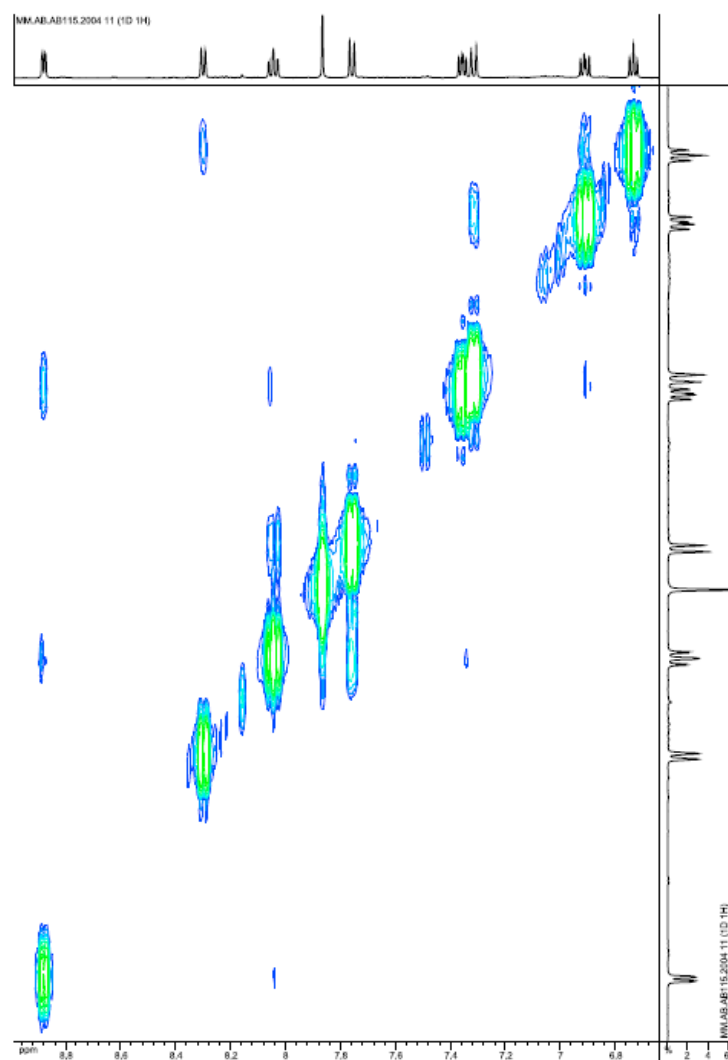


**Figure S5.** <sup>1</sup>H-<sup>1</sup>H ROESY NMR spectrum recorded for complex **1** in  $\text{CD}_2\text{Cl}_2$  at 298 K.

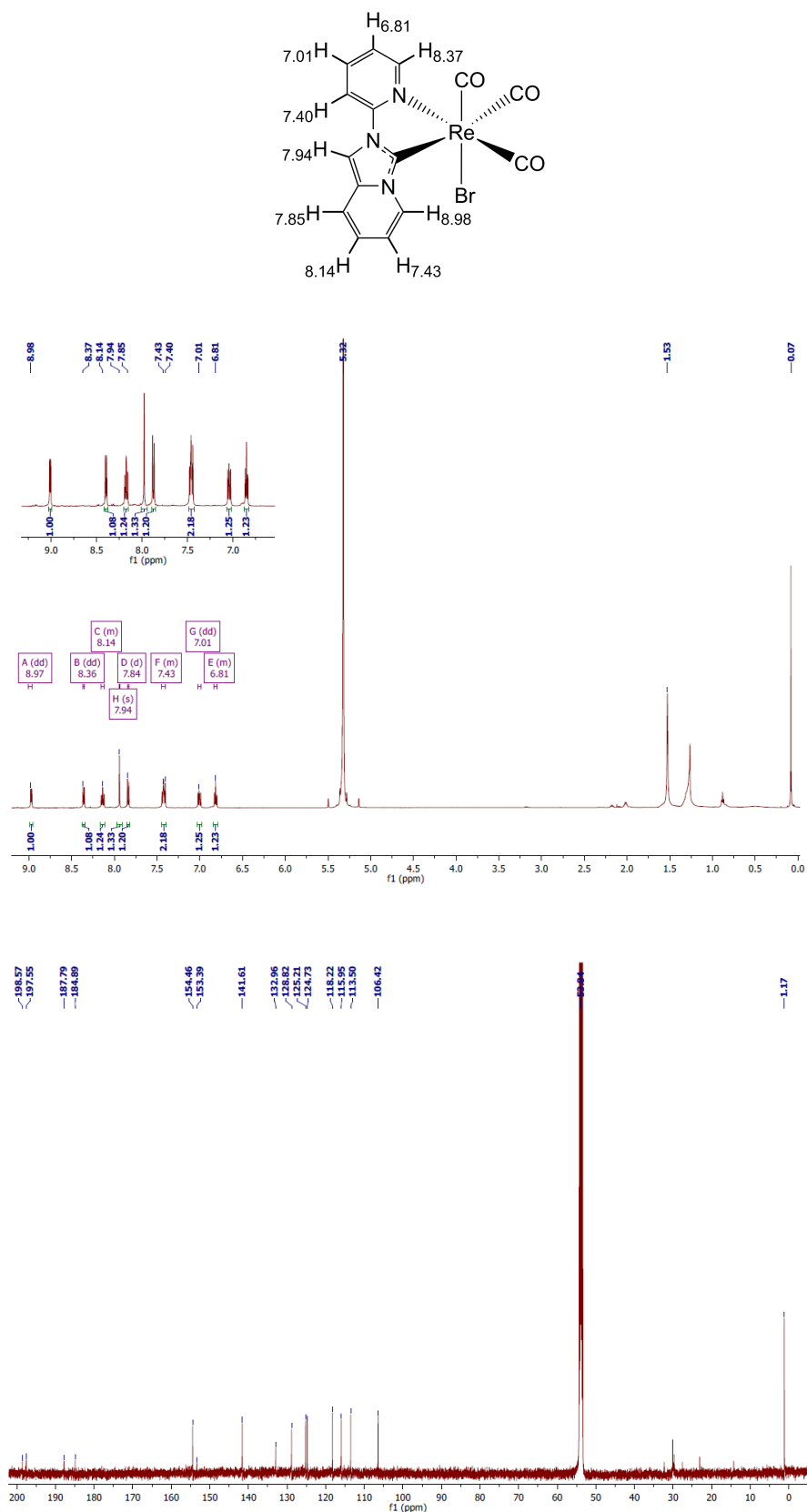


**Figure S6.** <sup>1</sup>H (500 MHz, *top*) and <sup>13</sup>C NMR (125 MHz, *bottom*) spectra recorded for complex **2** in CD<sub>2</sub>Cl<sub>2</sub> at 298 K.

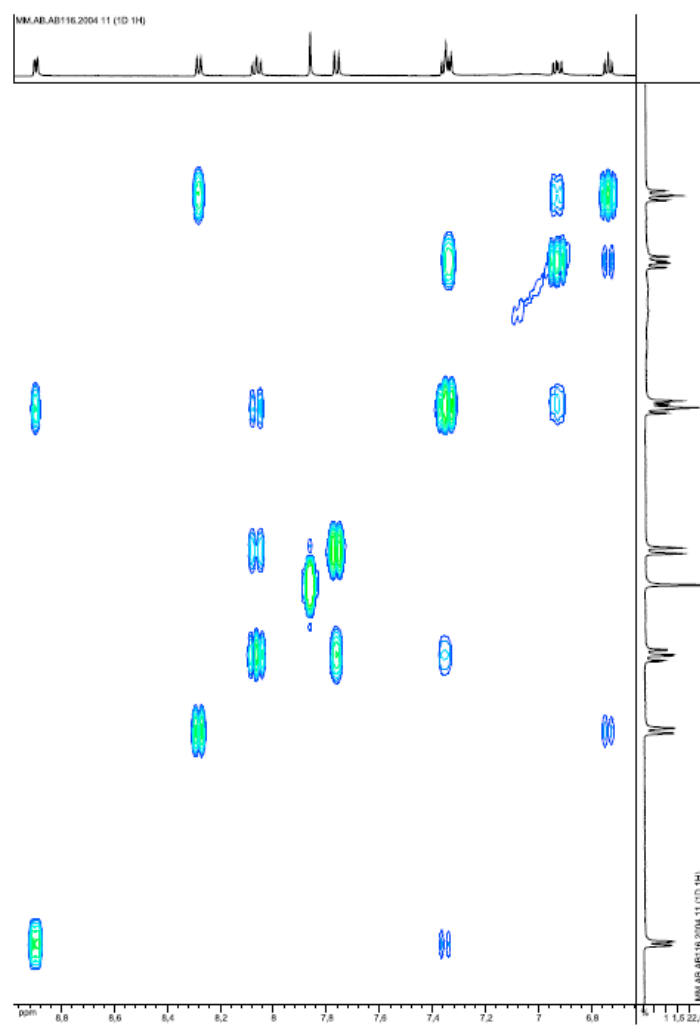


**Figure S7.**  $^1\text{H}$ - $^1\text{H}$  COSY NMR spectrum recorded for complex **2** in  $\text{CD}_2\text{Cl}_2$  at 298 K.

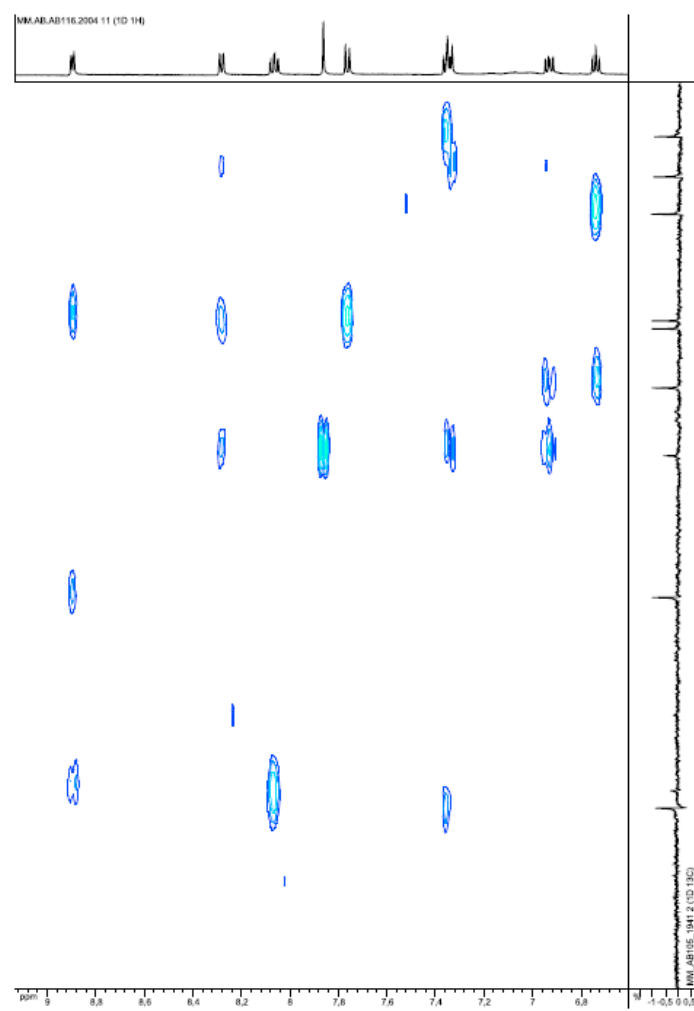


**Figure S8.**  $^1\text{H}$ - $^{13}\text{C}$  HMBC spectrum recorded for complex **2** in  $\text{CD}_2\text{Cl}_2$  at 298 K.

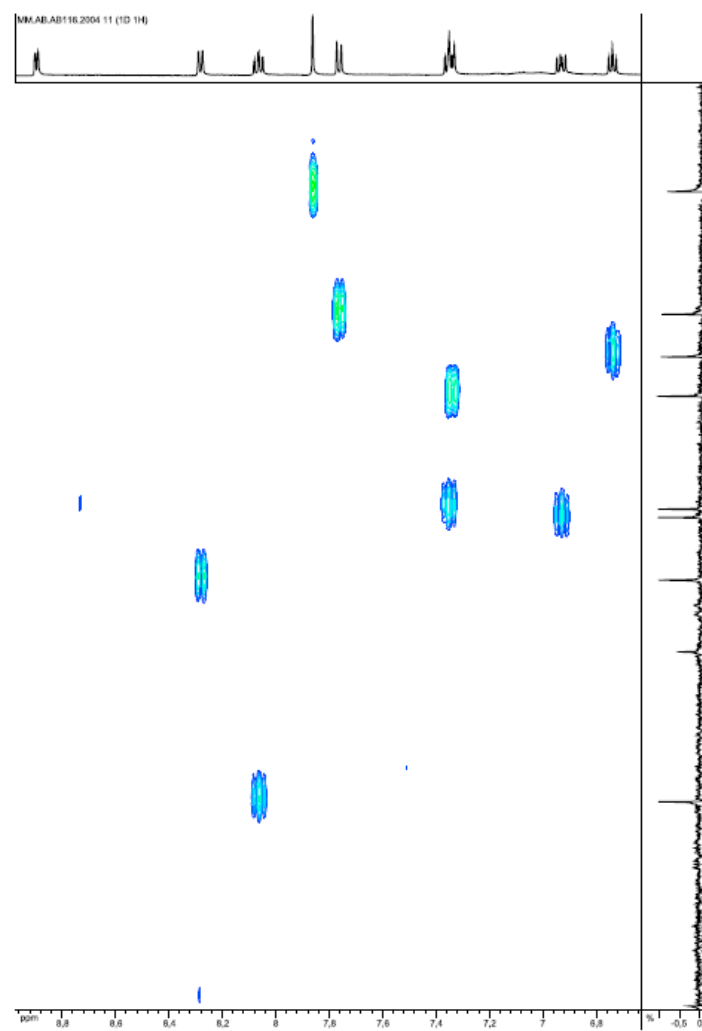


**Figure S9.**  $^1\text{H}$ - $^{13}\text{C}$  HSQC NMR spectrum recorded for complex **2** in  $\text{CD}_2\text{Cl}_2$  at 298 K.

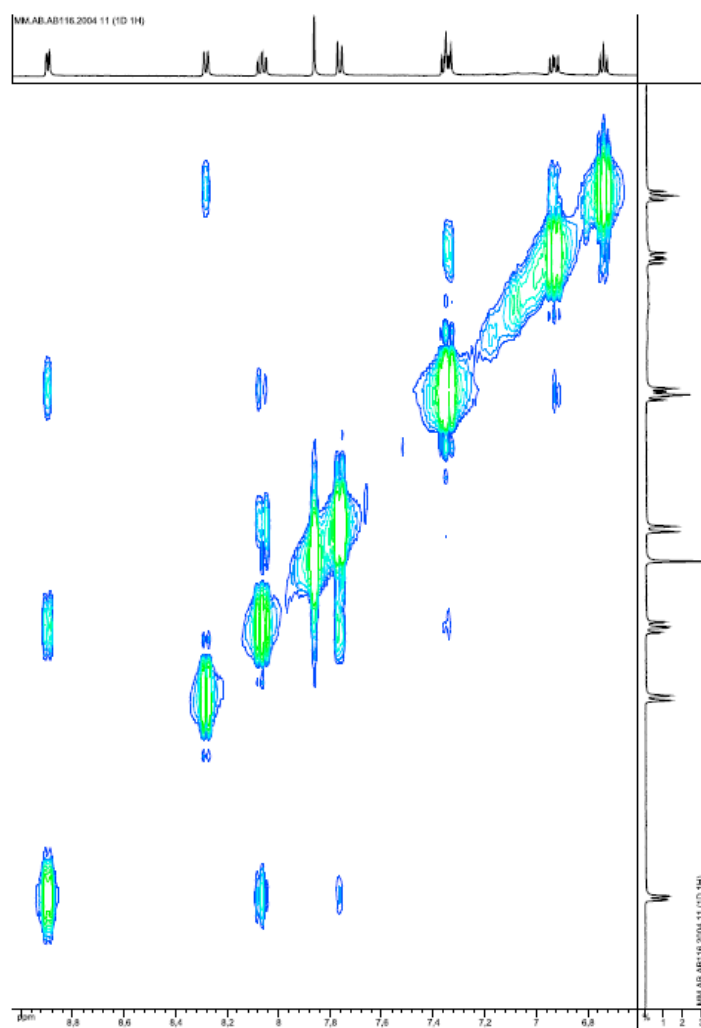


**Figure S10.**  $^1\text{H}$ - $^1\text{H}$  NOESY NMR spectrum recorded for complex **2** in  $\text{CD}_2\text{Cl}_2$  at 298 K.

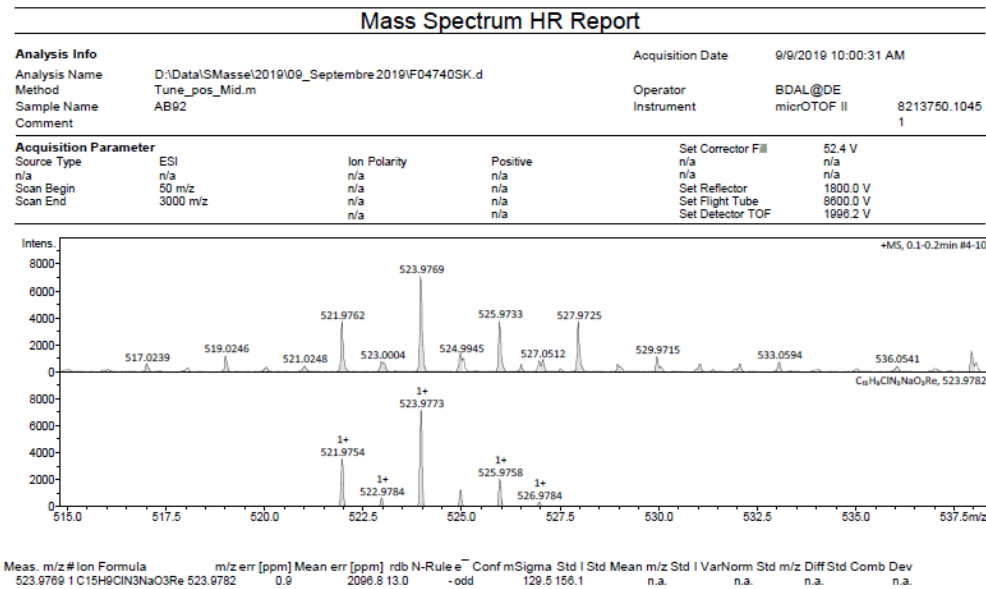


**Figure S11.** High-resolution ESI-MS spectrum of compound 1.

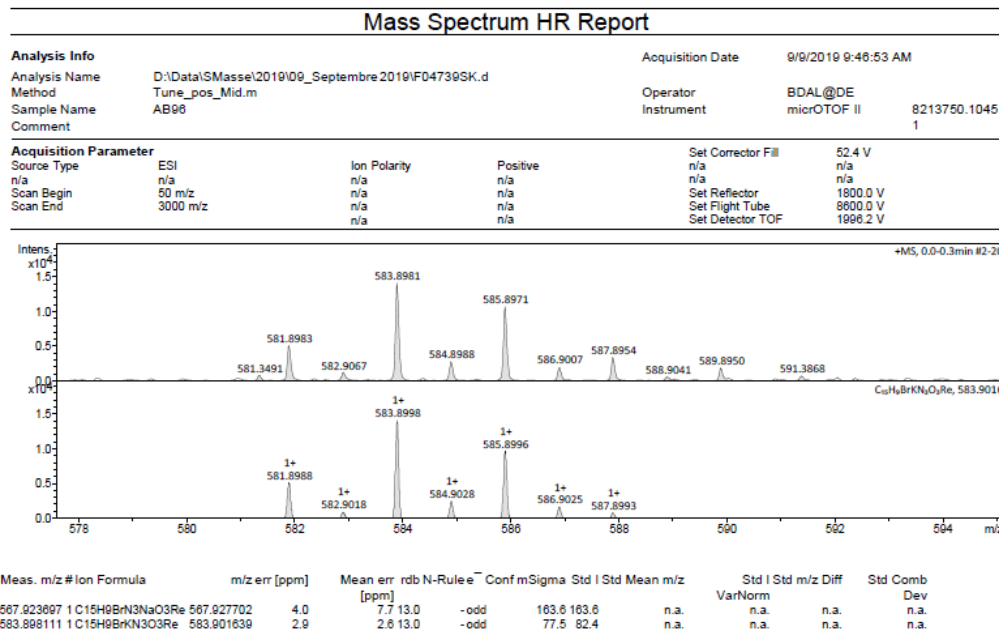


**Figure S12.** High-resolution ESI-MS spectrum of compound 2.

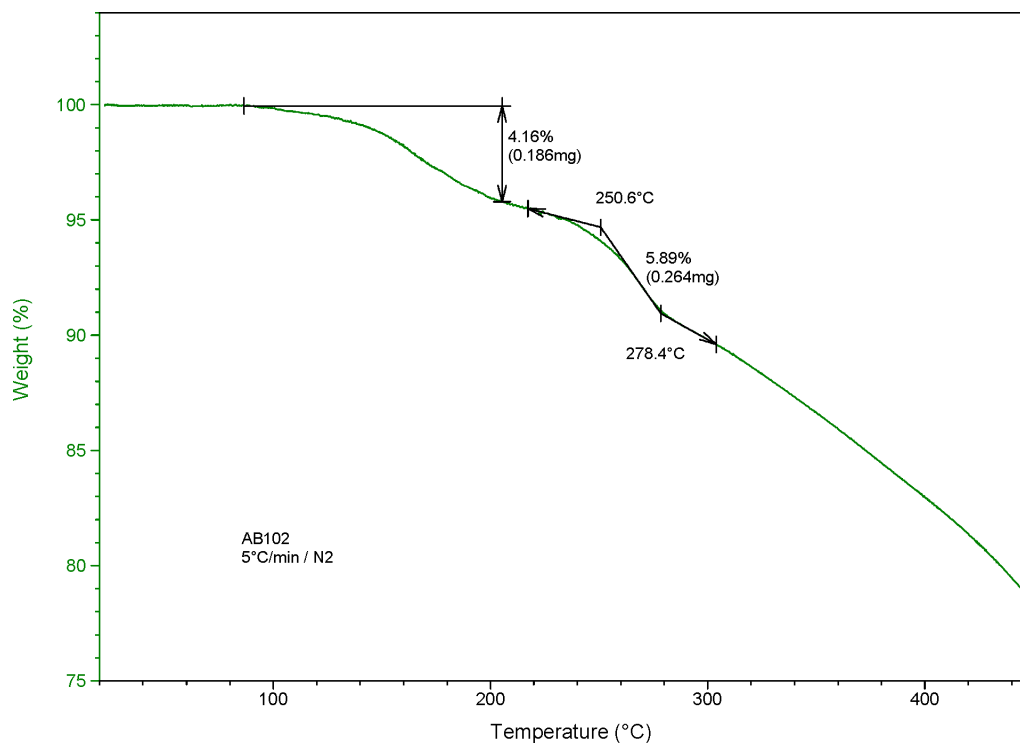


**Figure S13.** Thermogravimetric analysis recorded for complex **1**.

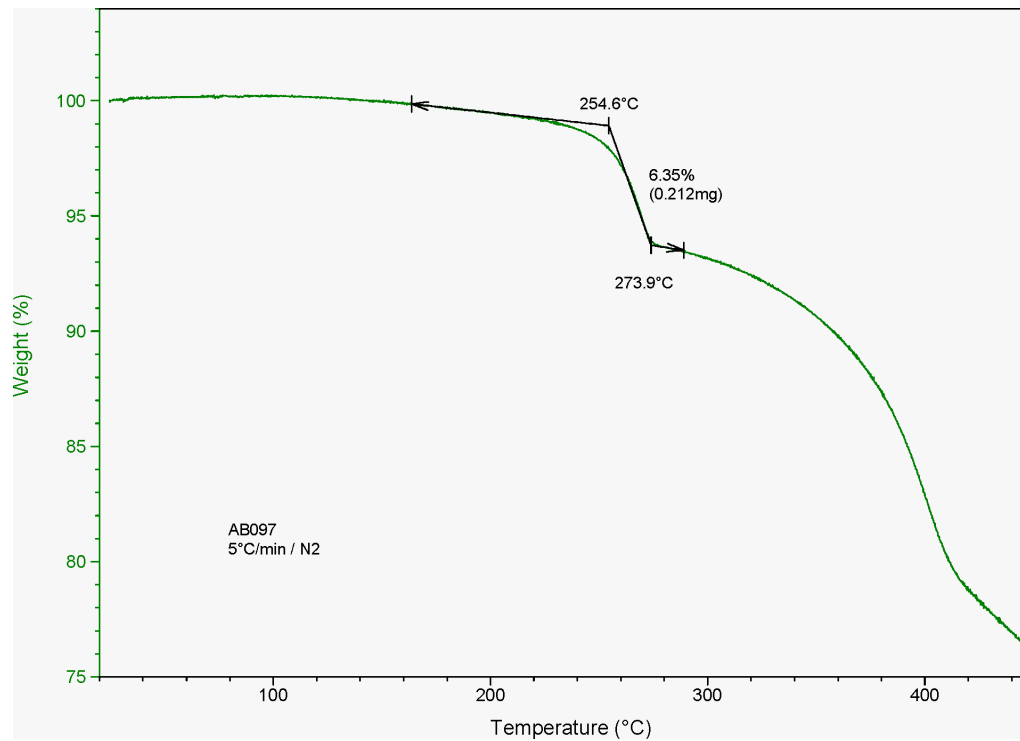


**Figure S14.** Thermogravimetric analysis recorded for complex **2**.

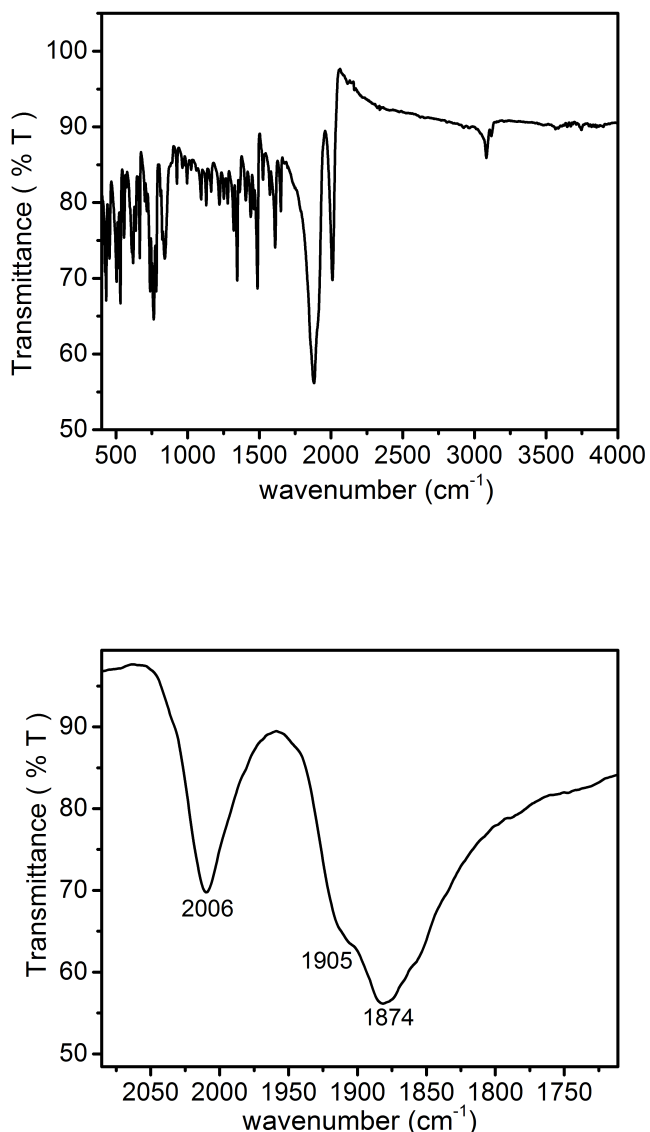


**Figure S15.** FT-ATR-IR spectra obtained for complex **1** in solid state as neat powder in the region  $4000 - 400 \text{ cm}^{-1}$  (*top*) and enlarged spectrum in the  $\nu\text{C}\equiv\text{O}$  region  $2085 - 1711 \text{ cm}^{-1}$  (*bottom*).

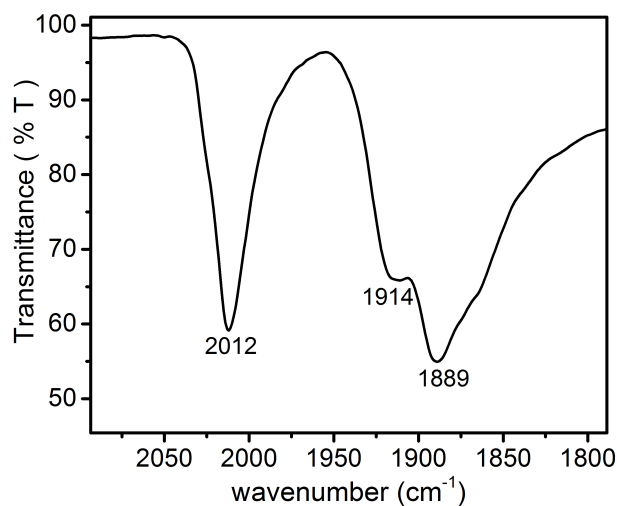
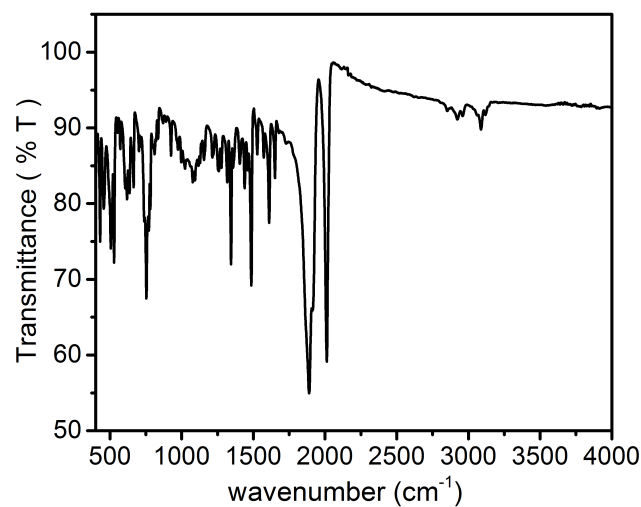


**Figure S16.** FT-ATR-IR spectra obtained for complex **2** in solid state as neat powder in the region  $4000 - 400\text{ cm}^{-1}$  (*top*) and enlarged spectrum in the  $\nu\text{C}\equiv\text{O}$  region  $2093 - 1788\text{ cm}^{-1}$  (*bottom*).

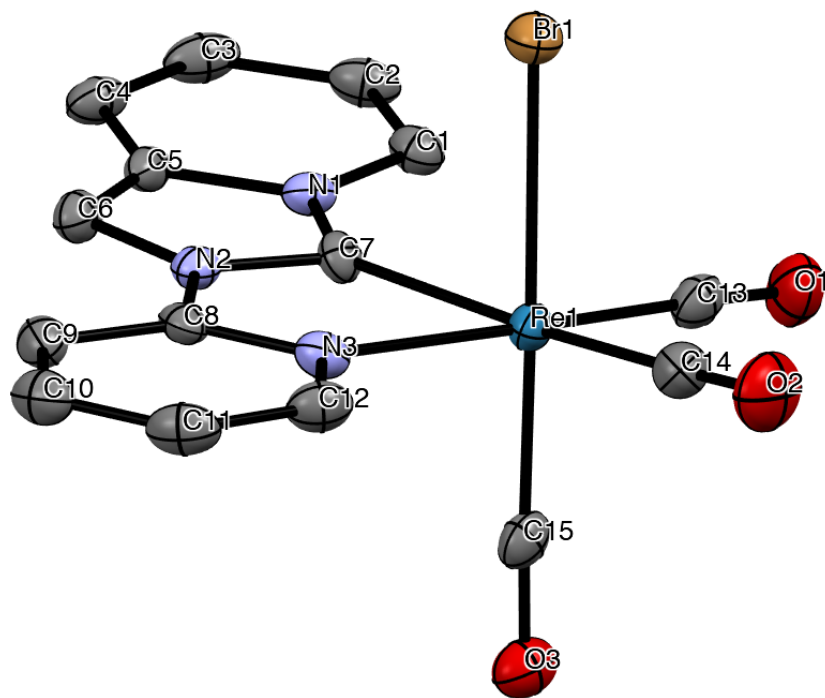


**Figure S17.** ORTEP diagram of compound **2** with thermal ellipsoids shown at 50% probability level obtained by single-crystal X-ray diffractometric analysis. Hydrogen atoms are omitted for clarity. Selected bond lengths (Å): Re–C(7) = 2.129(4) Å; Re–C(13) = 1.915(5) Å, Re–C(14) = 1.951(5) Å, Re–C(15) = 1.910(5) Å, Re–N(3) = 2.208(4) Å; Re–Br(1) = 2.6199(5) Å.

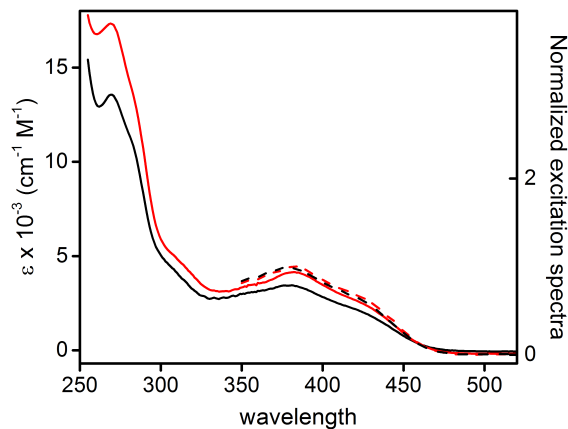


**Figure S18.** Electronic absorption (solid line) and normalized excitation spectra (dashed line) of complex **1** (black traces) and **2** (red traces) in degassed  $\text{CH}_2\text{Cl}_2$  solution at a concentration of  $2 \times 10^{-5}$  M at room temperature. Excitation spectra were recorded setting emission at  $\lambda_{\text{em}} = 660$  nm.

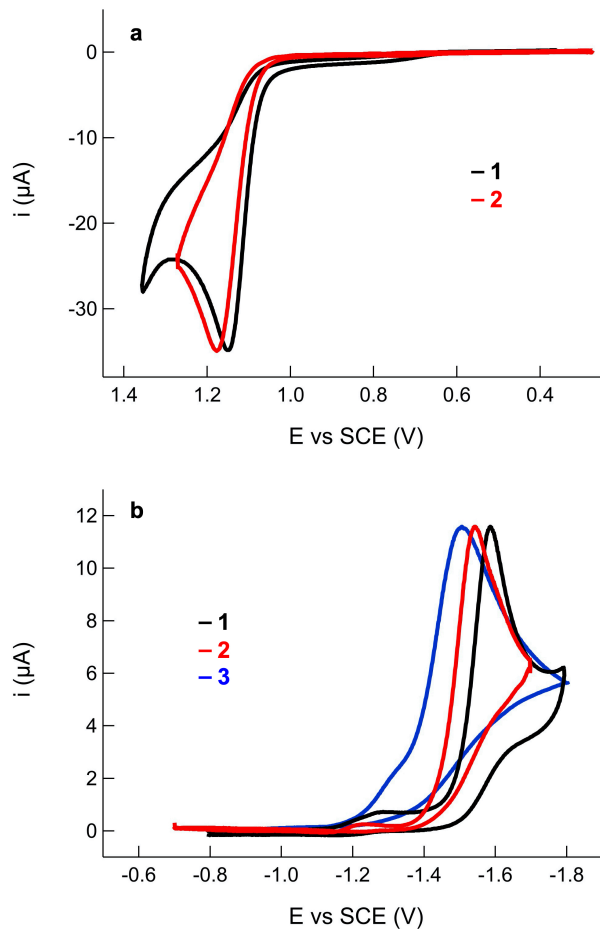


**Figure S19.** Blank-subtracted CVs recorded for 1 mM of compounds **1** (trace 1), compound **2** (trace 2) and ligand  $[\text{pyipy}] \text{PF}_6$  (trace 3) in DMF/0.1 M TBAP. Scan rate:  $0.1 \text{ V s}^{-1}$ . (a) anodic and (b) cathodic processes.

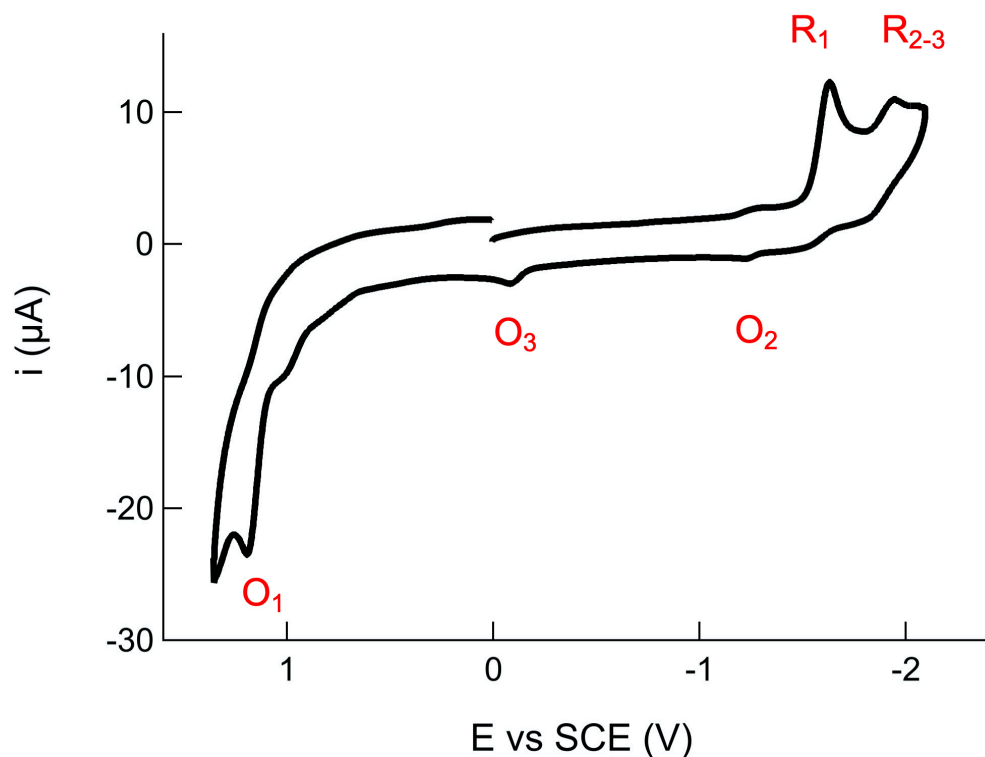


**Figure S20.** Full range CV of 1 mM **1** in DMF/0.1 M TBAP covering both the reduction and oxidation processes. Scan rate: 0.1 V s<sup>-1</sup>.

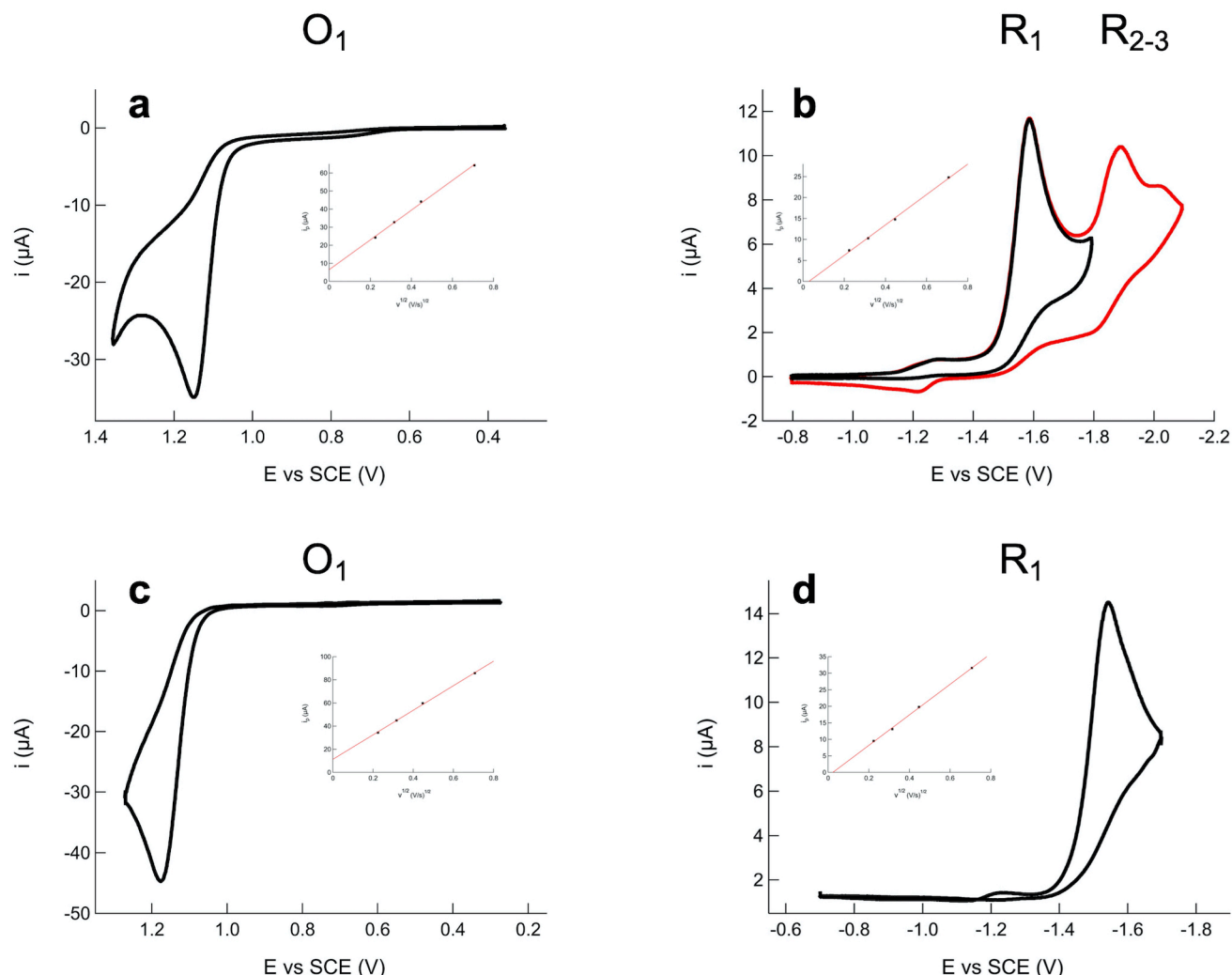


**Figure S21.** CVs in DMF/0.1 M TBAP showing the oxidation (a) and reduction (b) processes of 1 mM **1**, and the oxidation (c) and reduction processes (d) of 1 mM **2**. The insets provide the electrochemical analyses (peak current,  $i_p$ , vs the square root of the scan rate,  $v^{1/2}$ ) assessing the diffusion-controlled regime of the redox processes. The redox process for **1** in the negative bias covering also  $R_2$  and  $R_3$  is also shown (red line, b).

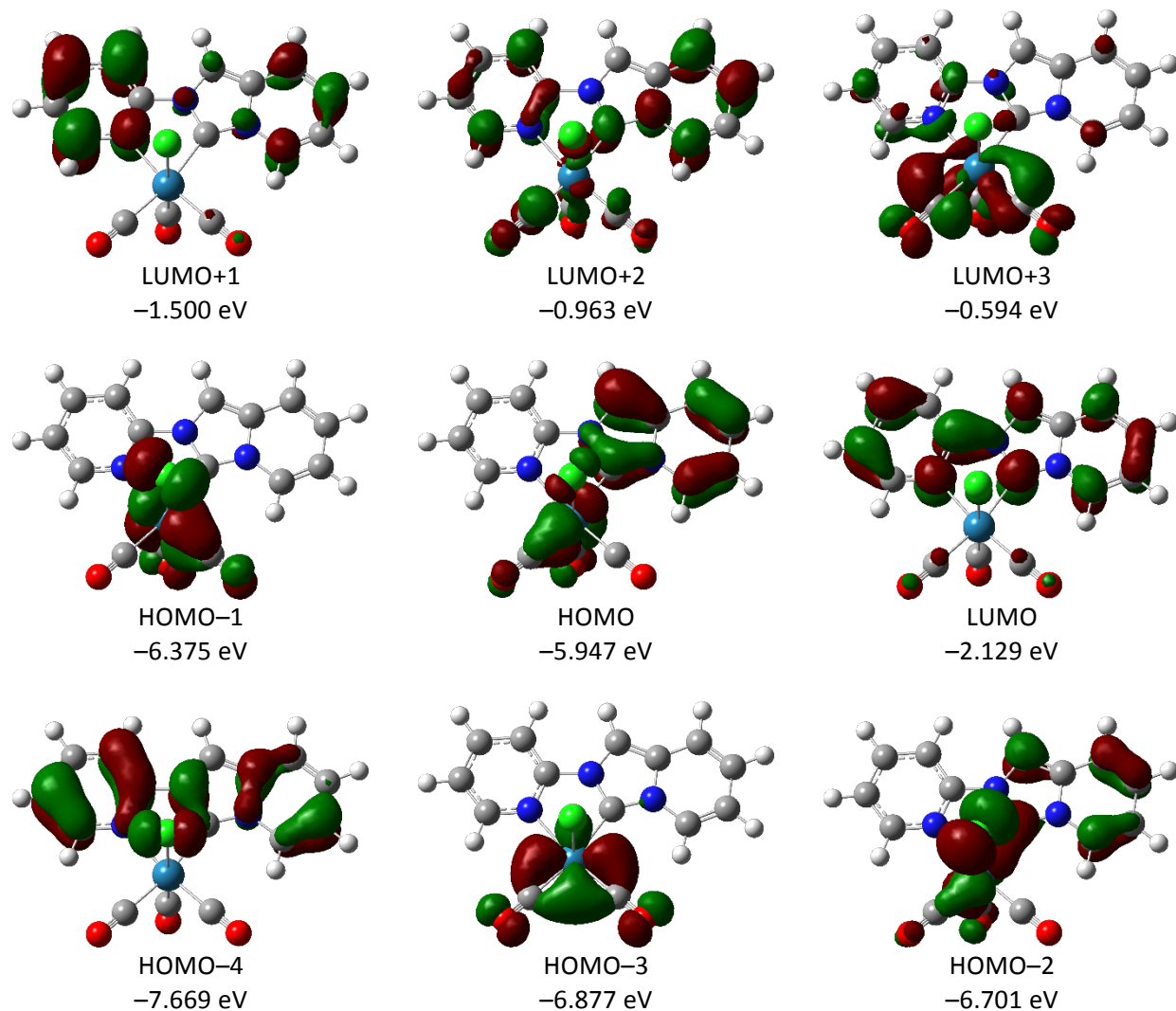


**Figure S22.** Isodensity surface plots and energies computed for some relevant molecular orbitals of *fac*-[Re(pyipy)(CO)<sub>3</sub>Cl] (**1**).

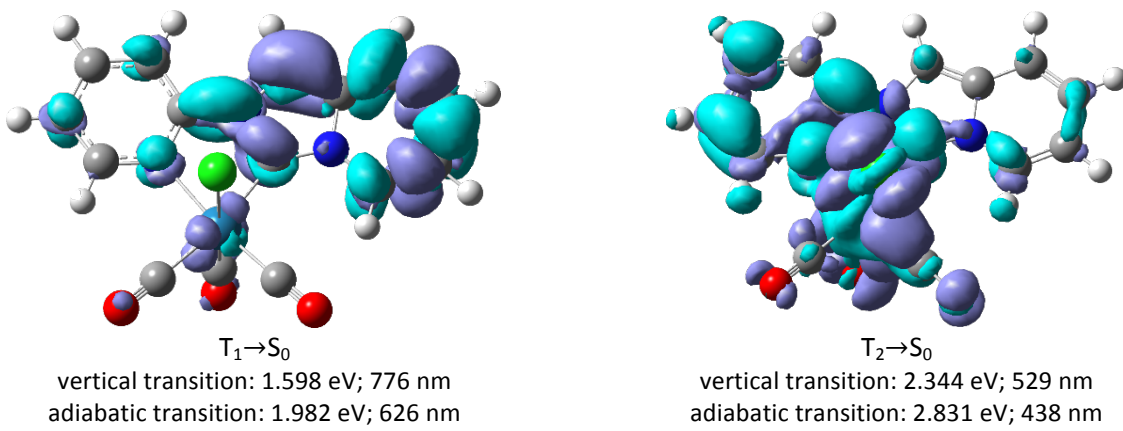


**Figure S23.** Electronic density difference maps computed (at the optimized geometry of the corresponding triplet) for the vertical transition  $T_1 \rightarrow S_0$  and  $T_2 \rightarrow S_0$  of *fac*-[Re(pyipy)(CO)<sub>3</sub>Cl] (**1**). Energy computed for the corresponding adiabatic transition is also reported. The difference in energy between the  $T_1$  and  $T_2$  minima is 31.210 mE<sub>h</sub> (0.849 eV; 6850 cm<sup>-1</sup>).

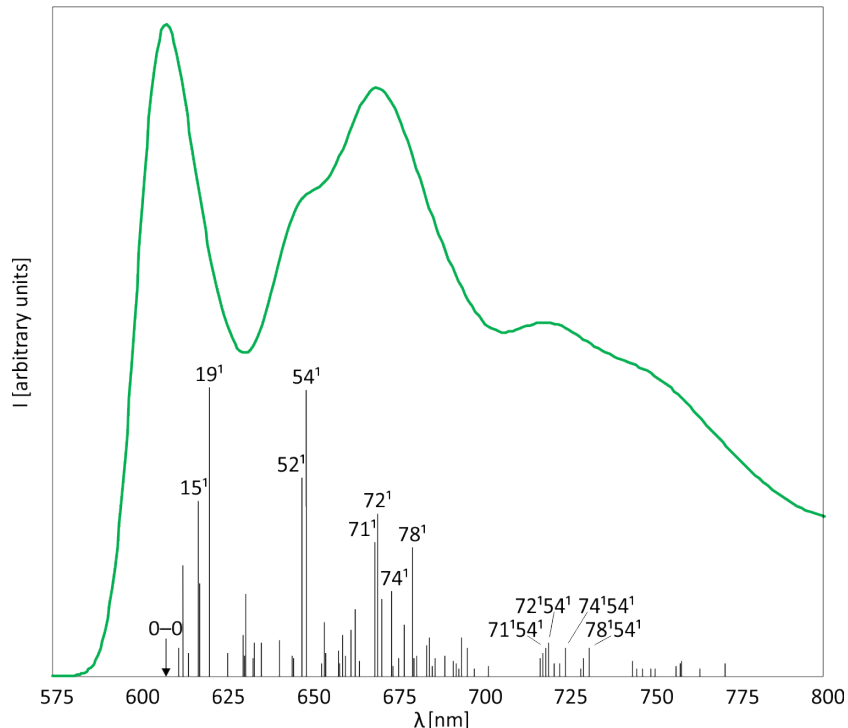


**Figure S24.** Assignment of the main bands of the computed emission spectrum of the  $T_1 \rightarrow S_0$  electronic transition of *fac*-[Re(pyipy)(CO)<sub>3</sub>Cl] (**1**). The solid line reports the harmonic spectrum calculated within the Franck-Condon approximation (half-width at half-maximum set to 220 cm<sup>-1</sup>) and the sticks are labelled as  $\nu^x$  where  $\nu$  is the ground state normal mode and  $x$  its quantum number.

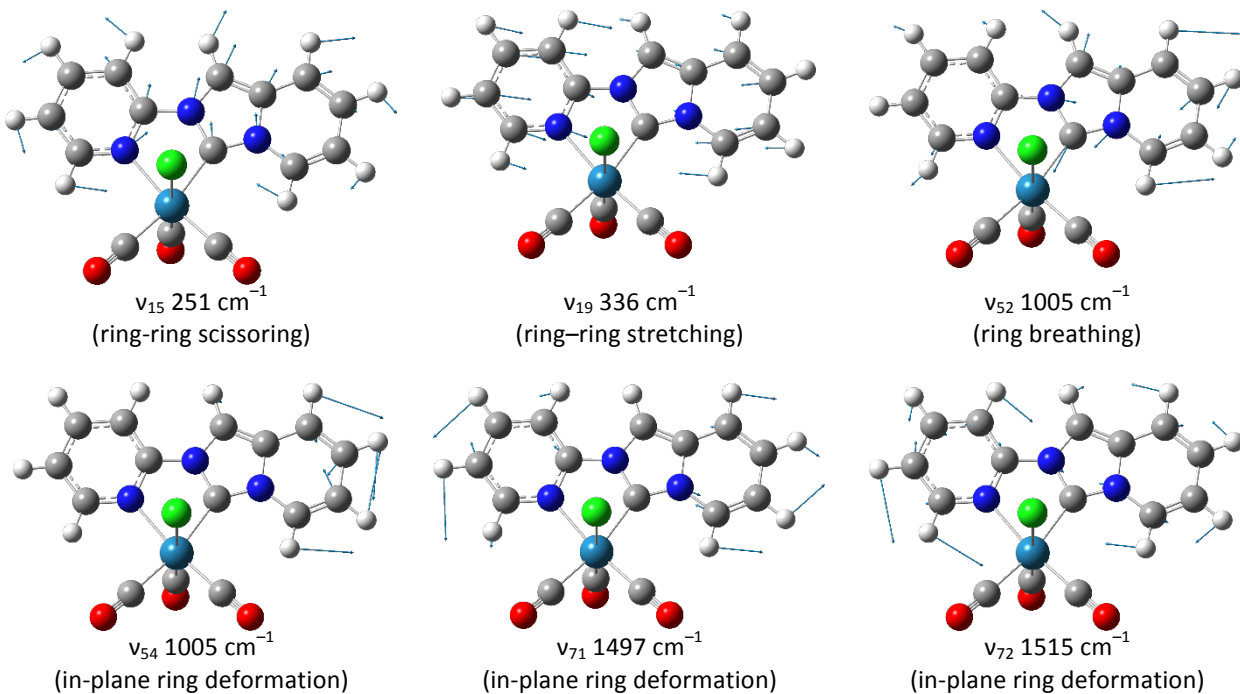


**Figure S25.** Some relevant normal modes computed for the ground state of *fac*-[Re(pyipy)(CO)<sub>3</sub>Cl] (**1**).

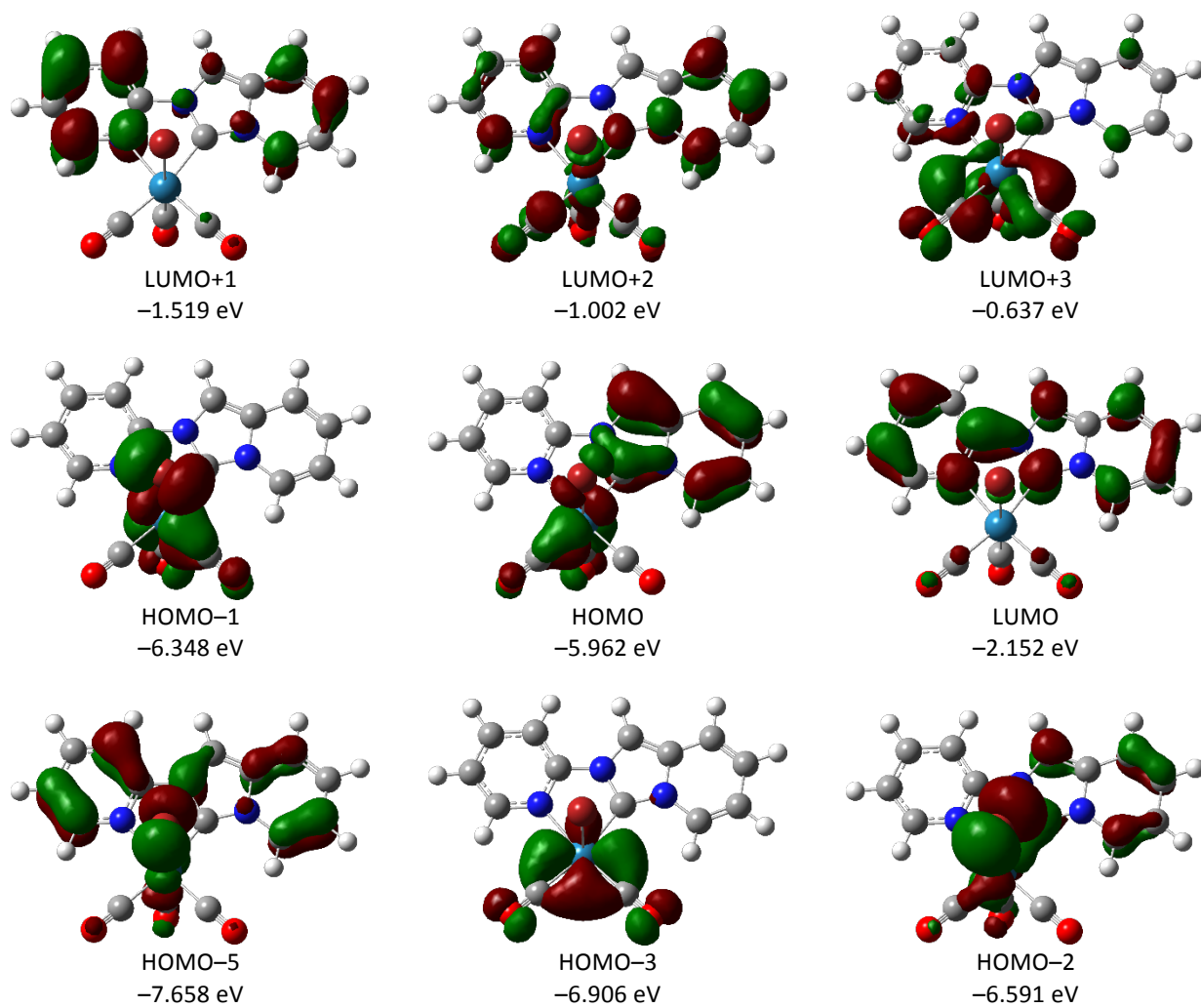


**Figure S26.** Isodensity surface plots and energies computed for some relevant molecular orbitals of *fac*-[Re(pyipy)(CO)<sub>3</sub>Br] (**2**).

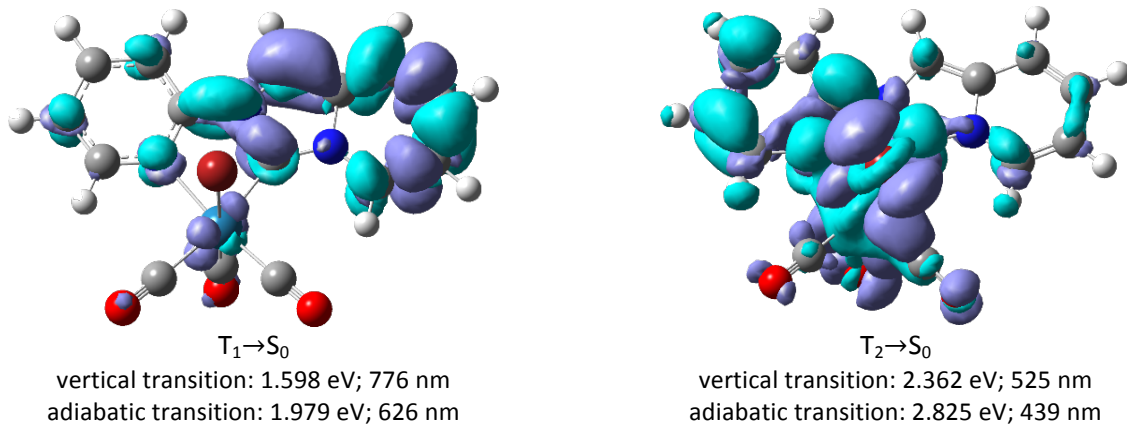


**Figure S27.** Electronic density difference maps computed (at the optimized geometry of the corresponding triplet) for the vertical transition  $T_1 \rightarrow S_0$  and  $T_2 \rightarrow S_0$  of *fac*-[Re(pypi)(CO)<sub>3</sub>Br] (**2**). Energy computed for the corresponding adiabatic transition is also reported. The difference in energy between the  $T_1$  and  $T_2$  minima is 31.088 mE<sub>h</sub> (0.846 eV; 6823 cm<sup>-1</sup>). Cyan and violet indicates a decrease and increase in electron density, respectively.

**Table S1.** Crystal data and structure refinement for compound **1**.

Identification code	CCDC 1973530
Empirical formula	C15 H9 Cl N3 O3 Re
Formula weight	500.90
Temperature	120(2) K
Wavelength	0.71073 Å
Crystal system, space group	Triclinic, P -1
Unit cell dimensions	$a = 6.6594(2)$ Å $\alpha = 89.3060(10)^\circ$ $b = 10.8376(4)$ Å $\beta = 77.6610(10)^\circ$ $c = 11.1557(4)$ Å $\gamma = 72.2660(10)^\circ$
Volume	747.94(4) Å <sup>3</sup>
Z, Calculated density	2, 2.224 Mg/m <sup>3</sup>
Absorption coefficient	8.319 mm <sup>-1</sup>
<i>F</i> (000)	472
Crystal size	0.200 x 0.150 x 0.120 mm
Theta range for data collection	1.976 to 30.076 deg.
Limiting indices	-9<=h<=9, -15<=k<=13, -15<=l<=15
Reflections collected / unique	54563 / 4399 [R(int) = 0.0367]
Completeness to theta = 25.242	99.9%
Absorption correction	Semi-empirical from equivalents
Max. and min. transmission	0.7460 and 0.6059
Refinement method	Full-matrix least-squares on <i>F</i> <sup>2</sup>
Data / restraints / parameters	4399 / 0 / 208
Goodness-of-fit on <i>F</i> <sup>2</sup>	1.106
Final R indices [ <i>I</i> >2σ( <i>I</i> )]	<i>R</i> 1 = 0.0152, w <i>R</i> 2 = 0.0302
R indices (all data)	<i>R</i> 1 = 0.0163, w <i>R</i> 2 = 0.0305
Extinction coefficient	n/a
Largest diff. peak and hole	1.616 and -0.985 e Å <sup>-3</sup>

**Table S2.** Geometrical parameters obtained for compound **1** by means of X-ray crystallographic analysis.

## Bond lengths [Å]

C(1)-C(2)	1.347(3)
C(1)-N(1)	1.396(3)
C(1)-H(1)	0.9500
C(2)-C(3)	1.437(3)
C(2)-H(2)	0.9500
C(3)-C(4)	1.353(3)
C(3)-H(3)	0.9500
C(4)-C(5)	1.425(3)
C(4)-H(4)	0.9500
C(5)-C(6)	1.365(3)
C(5)-N(1)	1.415(3)
C(6)-N(2)	1.387(2)
C(6)-H(6)	0.9500
C(7)-N(1)	1.359(3)
C(7)-N(2)	1.370(3)
C(7)-Re(1)	2.126(2)
C(8)-N(3)	1.342(3)
C(8)-C(9)	1.386(3)
C(8)-N(2)	1.411(3)
C(9)-C(10)	1.384(3)
C(9)-H(9)	0.9500
C(10)-C(11)	1.389(3)
C(10)-H(10)	0.9500
C(11)-C(12)	1.378(3)
C(11)-H(11)	0.9500
C(12)-N(3)	1.358(3)
C(12)-H(12)	0.9500
C(13)-O(1)	1.156(3)
C(13)-Re(1)	1.913(2)
C(14)-O(2)	1.145(3)
C(14)-Re(1)	1.957(2)
C(15)-O(3)	1.147(3)
C(15)-Re(1)	1.914(2)
N(3)-Re(1)	2.2085(17)
Cl(1)-Re(1)	2.5049(5)

## Bond angles [°]

C(2)-C(1)-N(1)	119.1(2)
C(2)-C(1)-H(1)	120.5
N(1)-C(1)-H(1)	120.5
C(1)-C(2)-C(3)	121.3(2)
C(1)-C(2)-H(2)	119.4
C(3)-C(2)-H(2)	119.4
C(4)-C(3)-C(2)	120.5(2)
C(4)-C(3)-H(3)	119.8
C(2)-C(3)-H(3)	119.8
C(3)-C(4)-C(5)	119.3(2)
C(3)-C(4)-H(4)	120.3
C(5)-C(4)-H(4)	120.3
C(6)-C(5)-N(1)	106.30(17)
C(6)-C(5)-C(4)	134.8(2)
N(1)-C(5)-C(4)	118.85(19)
C(5)-C(6)-N(2)	105.53(17)

C(5)-C(6)-H(6)	127.2
N(2)-C(6)-H(6)	127.2
N(1)-C(7)-N(2)	102.88(16)
N(1)-C(7)-Re(1)	140.64(15)
N(2)-C(7)-Re(1)	116.36(14)
N(3)-C(8)-C(9)	124.18(19)
N(3)-C(8)-N(2)	113.63(17)
C(9)-C(8)-N(2)	122.18(18)
C(10)-C(9)-C(8)	117.66(19)
C(10)-C(9)-H(9)	121.2
C(8)-C(9)-H(9)	121.2
C(9)-C(10)-C(11)	119.5(2)
C(9)-C(10)-H(10)	120.2
C(11)-C(10)-H(10)	120.2
C(12)-C(11)-C(10)	118.9(2)
C(12)-C(11)-H(11)	120.5
C(10)-C(11)-H(11)	120.5
N(3)-C(12)-C(11)	122.7(2)
N(3)-C(12)-H(12)	118.6
C(11)-C(12)-H(12)	118.6
O(1)-C(13)-Re(1)	176.2(2)
O(2)-C(14)-Re(1)	177.1(2)
O(3)-C(15)-Re(1)	178.6(2)
C(7)-N(1)-C(1)	127.11(18)
C(7)-N(1)-C(5)	111.86(17)
C(1)-N(1)-C(5)	120.99(17)
C(7)-N(2)-C(6)	113.41(17)
C(7)-N(2)-C(8)	118.68(17)
C(6)-N(2)-C(8)	127.90(17)
C(8)-N(3)-C(12)	116.99(18)
C(8)-N(3)-Re(1)	117.26(13)
C(12)-N(3)-Re(1)	125.64(14)
C(13)-Re(1)-C(15)	87.28(9)
C(13)-Re(1)-C(14)	89.70(9)
C(15)-Re(1)-C(14)	91.94(9)
C(13)-Re(1)-C(7)	100.48(9)
C(15)-Re(1)-C(7)	94.99(8)
C(14)-Re(1)-C(7)	167.92(9)
C(13)-Re(1)-N(3)	173.71(8)
C(15)-Re(1)-N(3)	90.34(8)
C(14)-Re(1)-N(3)	96.20(8)
C(7)-Re(1)-N(3)	73.92(7)
C(13)-Re(1)-Cl(1)	95.95(7)
C(15)-Re(1)-Cl(1)	176.71(7)
C(14)-Re(1)-Cl(1)	87.46(7)
C(7)-Re(1)-Cl(1)	85.05(5)
N(3)-Re(1)-Cl(1)	86.51(5)

**Table S3.** Crystal data and structure refinement for compound **2**.

Identification code	CCDC 1980932
Empirical formula	C15 H9 Br N3 O3 Re
Formula weight	545.36
Temperature	120(2) K
Wavelength	0.71073 Å
Crystal system, space group	Triclinic, P -1
Unit cell dimensions	$a = 6.7338(3)$ Å $\alpha = 88.7910(10)^\circ$ $b = 10.8986(4)$ Å $\beta = 76.4800(10)^\circ$ $c = 11.3120(5)$ Å $\gamma = 72.1440(10)^\circ$
Volume	767.14(6) Å <sup>3</sup>
Z, Calculated density	2, 2.361 Mg/m <sup>3</sup>
Absorption coefficient	10.542 mm <sup>-1</sup>
<i>F</i> (000)	508
Crystal size	0.180 x 0.150 x 0.120 mm
Theta range for data collection	1.966 to 29.168 deg.
Limiting indices	-9<=h<=9, -14<=k<=14, -15<=l<=15
Reflections collected / unique	54752 / 4137 [R(int) = 0.0597]
Completeness to theta = 25.242	100.0 %
Absorption correction	Semi-empirical from equivalents
Max. and min. transmission	0.7458 and 0.5741
Refinement method	Full-matrix least-squares on <i>F</i> <sup>2</sup>
Data / restraints / parameters	4137 / 0 / 208
Goodness-of-fit on <i>F</i> <sup>2</sup>	1.109
Final R indices [ <i>I</i> >2σ( <i>I</i> )]	<i>R</i> 1 = 0.0295, <i>wR</i> 2 = 0.0621
R indices (all data)	<i>R</i> 1 = 0.0342, <i>wR</i> 2 = 0.0649
Extinction coefficient	n/a
Largest diff. peak and hole	3.362 and -1.941 e Å <sup>-3</sup>

**Table S4.** Geometrical parameters obtained for compound **2** by means of X-ray crystallographic analysis.

## Bond lengths [Å]

C(1)-C(2)	1.347(7)
C(1)-N(1)	1.396(6)
C(1)-H(1)	0.9500
C(2)-C(3)	1.440(8)
C(2)-H(2)	0.9500
C(3)-C(4)	1.339(8)
C(3)-H(3)	0.9500
C(4)-C(5)	1.428(7)
C(4)-H(4)	0.9500
C(5)-C(6)	1.359(7)
C(5)-N(1)	1.416(6)
C(6)-N(2)	1.384(6)
C(6)-H(6)	0.9500
C(7)-N(1)	1.349(6)
C(7)-N(2)	1.374(6)
C(7)-Re(1)	2.129(4)
C(8)-N(3)	1.344(6)
C(8)-C(9)	1.381(7)
C(8)-N(2)	1.411(6)
C(9)-C(10)	1.385(7)
C(9)-H(9)	0.9500
C(10)-C(11)	1.382(8)
C(10)-H(10)	0.9500
C(11)-C(12)	1.380(8)
C(11)-H(11)	0.9500
C(12)-N(3)	1.355(6)
C(12)-H(12)	0.9500
C(13)-O(1)	1.154(6)
C(13)-Re(1)	1.915(5)
C(14)-O(2)	1.150(6)
C(14)-Re(1)	1.951(5)
C(15)-O(3)	1.146(6)
C(15)-Re(1)	1.910(5)
N(3)-Re(1)	2.208(4)
Br(1)-Re(1)	2.6199(5)

## Bond angles [°]

C(2)-C(1)-N(1)	118.6(5)
C(2)-C(1)-H(1)	120.7
N(1)-C(1)-H(1)	120.7
C(1)-C(2)-C(3)	121.2(5)
C(1)-C(2)-H(2)	119.4
C(3)-C(2)-H(2)	119.4
C(4)-C(3)-C(2)	121.0(5)

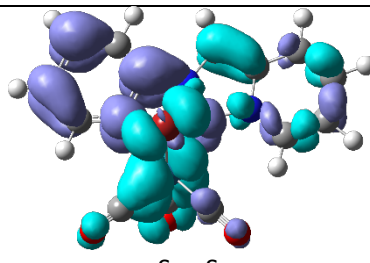
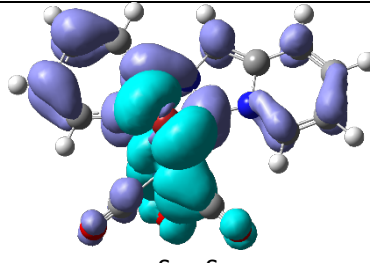
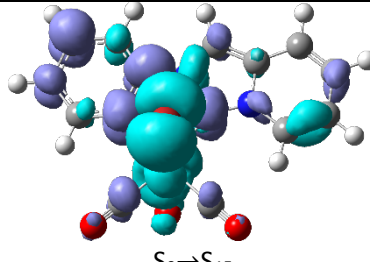
C(4)-C(3)-H(3)	119.5
C(2)-C(3)-H(3)	119.5
C(3)-C(4)-C(5)	119.3(5)
C(3)-C(4)-H(4)	120.4
C(5)-C(4)-H(4)	120.4
C(6)-C(5)-N(1)	106.2(4)
C(6)-C(5)-C(4)	135.2(5)
N(1)-C(5)-C(4)	118.6(5)
C(5)-C(6)-N(2)	106.0(4)
C(5)-C(6)-H(6)	127.0
N(2)-C(6)-H(6)	127.0
N(1)-C(7)-N(2)	103.3(4)
N(1)-C(7)-Re(1)	140.7(3)
N(2)-C(7)-Re(1)	115.8(3)
N(3)-C(8)-C(9)	124.7(4)
N(3)-C(8)-N(2)	113.2(4)
C(9)-C(8)-N(2)	122.1(4)
C(8)-C(9)-C(10)	117.5(5)
C(8)-C(9)-H(9)	121.2
C(10)-C(9)-H(9)	121.2
C(11)-C(10)-C(9)	119.4(5)
C(11)-C(10)-H(10)	120.3
C(9)-C(10)-H(10)	120.3
C(12)-C(11)-C(10)	119.1(5)
C(12)-C(11)-H(11)	120.4
C(10)-C(11)-H(11)	120.4
N(3)-C(12)-C(11)	122.8(5)
N(3)-C(12)-H(12)	118.6
C(11)-C(12)-H(12)	118.6
O(1)-C(13)-Re(1)	177.5(5)
O(2)-C(14)-Re(1)	177.8(5)
O(3)-C(15)-Re(1)	177.9(5)
C(7)-N(1)-C(1)	126.8(4)
C(7)-N(1)-C(5)	111.8(4)
C(1)-N(1)-C(5)	121.4(4)
C(7)-N(2)-C(6)	112.7(4)
C(7)-N(2)-C(8)	119.3(4)
C(6)-N(2)-C(8)	128.0(4)
C(8)-N(3)-C(12)	116.4(4)
C(8)-N(3)-Re(1)	117.5(3)
C(12)-N(3)-Re(1)	126.0(3)
C(15)-Re(1)-C(13)	87.4(2)
C(15)-Re(1)-C(14)	91.9(2)
C(13)-Re(1)-C(14)	89.8(2)
C(15)-Re(1)-C(7)	95.33(19)
C(13)-Re(1)-C(7)	100.16(19)
C(14)-Re(1)-C(7)	167.9(2)
C(15)-Re(1)-N(3)	91.48(18)
C(13)-Re(1)-N(3)	174.05(18)
C(14)-Re(1)-N(3)	96.07(19)
C(7)-Re(1)-N(3)	74.11(16)

C(15)-Re(1)-Br(1)	177.35(16)
C(13)-Re(1)-Br(1)	95.01(15)
C(14)-Re(1)-Br(1)	87.03(15)
C(7)-Re(1)-Br(1)	85.31(12)
N(3)-Re(1)-Br(1)	86.22(10)

**Table S5.** Properties of some of the more intense electronic transitions computed for *fac*-[Re(pyipy)(CO)<sub>3</sub>Cl] (**1**). In the electronic density difference maps (EDDMs), cyan and violet indicates a decrease and increase in electron density, respectively.

$S_n$	$E$ [eV]	$\lambda$ [nm]	$f$				EDDM
1	2.982	416	0.0531	HOMO→LUMO	93%		
2	3.325	373	0.0641	HOMO-1→LUMO	92%		
14	4.679	265	0.1285	HOMO-4→LUMO HOMO-2→LUMO+2	55% 9%		
17	4.867	255	0.1033	HOMO-2→LUMO+2	72%		
21	5.138	241	0.1813	HOMO-2→LUMO+3 HOMO-6→LUMO HOMO→LUMO+5	34% 13% 9%		

**Table S6.** Properties of some of the more intense electronic transitions computed for *fac*-[Re(pyipy)(CO)<sub>3</sub>Br] (**2**). In the electronic density difference maps (EDDMs), cyan and violet indicates a decrease and increase in electron density, respectively.

$S_n$	$E$ [eV]	$\lambda$ [nm]	$f$				EDDM
1	2.975	417	0.0511	HOMO→LUMO	92%		
2	3.278	378	0.0524	HOMO-1→LUMO	92%		
15	4.616	269	0.0916	HOMO-5→LUMO HOMO-1→LUMO+2	71% 13%		
18	4.800	258	0.0901	HOMO-6→LUMO HOMO→LUMO+5	73% 10%		